

Optimisation and economics of solar cooling systems

Ursula Eicker, Dirk Pietruschka

University of Applied Sciences Stuttgart, Schellingstrasse 24, D-70174 Stuttgart

Tel +49 711 8926 2831, Fax +49 711 8926 2698, Email: ursula.eicker@hft-stuttgart.de

Abstract

In this paper, the two main market available thermal cooling technologies with regeneration temperatures below 100°C are evaluated. For closed cycle absorption chillers and open desiccant cooling systems, efficiencies, costs and optimisation potentials are analysed. Measurements and simulation studies from realised demonstration projects are presented. If properly designed, both technologies offer significant primary energy savings. However, as coefficients of performance are generally lower than for electrically driven compressor chillers, care has to be taken to reduce auxiliary energy demand. While measured average thermal COP's are between 0.6 and 0.7 for absorption chillers, desiccant units can reach higher values, as they often operate with evaporative cooling only. The electrical COP's can be as high as 11 for absorption systems with efficient cold distribution and recooling units and is about 7-8 for desiccant systems with an air based distribution system. The total costs of both desiccant and absorption cooling systems are dominated by capital costs so that high full load hours are crucial for an economic performance.

Introduction

Solar or waste heat driven thermal cooling plants can provide summer comfort conditions in buildings at low primary energy consumption. Today, the dominant cooling systems are electrically driven compression chillers, which have a world market share of about 90%. The average coefficient of performance (COP) of installed systems is about 3.0 or lower and only the best available equipment can reach an annual average COP above 5.0. To reduce the primary energy consumption of chillers, thermal cooling systems offer interesting alternatives, especially if primary energy neutral heat from solar thermal collectors or waste heat from cogeneration units can be used. The main technologies

for thermal cooling are closed cycle absorption and adsorption machines, which use either liquids or solids for the sorption process of the refrigerant. The useful cold is in both cases produced through the evaporation of the refrigerant in exact analogy to the electrical chillers. For air based cooling systems, desiccant cooling cycles are useful, as they directly condition the inlet air to the building.

Thermal cooling systems are mainly powered by waste heat or fossil fuel sources. In 2005, solar cooling systems in Europe had a total capacity of 6 MW only (Nick-Leptin, 2005).

The type of solar thermal collector required for the sorption material regeneration depends on the heating temperature level, which in closed systems is a function of both cold water and cooling water temperatures. In open sorption systems, the regeneration heating temperature depends on the required dehumidification rate, which is a function of ambient air conditions.

Commercial adsorption systems, either open air based systems or closed adsorption, are designed for heating temperature ranges around 70°C. Single effect absorption chillers start at operation temperatures of about 70°C. Commercial machines are often designed for average heating temperatures of 85 – 90° C.

For the often used single effect machines, the ratio of cold production to input heat (COP) is in the range of 0.5 – 0.8. Solar fractions therefore need to be higher than about 50% to start saving primary energy (Mendes et al, 1998). The exact value of the minimum solar fraction required for energy saving not only depends on the performance of the thermal chiller, but also on other components such as the cooling tower: a thermal cooling system with an energy efficient cooling tower performs better than a compression chiller at a solar fraction of 40%, a low efficiency cooling tower increases the required solar fraction to 63%. These values were calculated for a thermal chiller COP of 0.7, a compressor COP of 2.5 and an electricity consumption of the cooling tower between 0.02 or 0.08 kWh_{el} per kWh of cold (Henning, 2004).

Double effect absorption cycles have considerably higher COPs around 1.1 – 1.4, but require significantly higher driving temperatures between 120 and 170°C (Wardono and Nelson, 1996), so that the energetical and economical performance of the solar thermal cooling system is not necessarily better (Grossmann, 2002).

In recent years, the consideration of auxiliary energy consumption of thermal chiller systems has increased in importance. Due to the low COP's, the amount of rejected heat is significantly higher than for compression chillers, which requires additional electrical energy for pumps and fans as well as increased water consumption. Complete primary energy balances have to be established to compare the efficiency of thermal cooling technologies to purely electrical systems.

As the focus of this work is on solar driven thermal chillers, the optimum use of the fluctuating solar energy source has to be analysed. This issue mainly concerns control strategies, which are responsible for auxiliary energy system setpoints, shortening of start-up times in the morning with rising irradiance and storage management in general. These aspects will be discussed in the paper.

Based on measurements and simulation results from solar cooling systems, the energetic and economical performance of solar powered absorption and desiccant cooling systems will be presented. The goals are to analyse the solar contribution to the total energy demand of the thermal chiller system and to specify the associated costs.

Technology overview absorption cooling

Absorption cooling is a mature technology with the first machine developed in 1859 by Ferdinand Carré. For the closed cycle process, a binary working fluid that consists of the refrigerant and an absorbent is necessary. Carré used the working fluid ammonia/water ($\text{NH}_3/\text{H}_2\text{O}$). Today the working pair Lithium bromide as absorbent and water as the refrigerant is most commonly used for building climatisation ($\text{H}_2\text{O}/\text{LiBr}$). In contrast to the ammonia/water system with its pressure levels above ambient pressure, the water/lithium bromide ACM works under vacuum because of the low vapour pressure of the refrigerant water.

In 1945 the company Carrier Corp, USA, developed and introduced the first large commercial single-effect absorption cooling machine (ACM) using water/lithium bromide with a cooling power of 523 kW. In 1964 the company Kawasaki Heavy Industry Co., Japan produced the first double effect water/lithium bromide ACM (Hartmann, 1992). The double-effect (DE) ACM is equipped with a second generator and condenser to increase the overall COP by re-using the high temperature input heat also for the lower temperature generator. Absorption chillers today are available in a range of

10 kW to 20 000 kW. In the last few years some new developments were made in the medium scale cooling range of 10 kW to 50 kW for water/lithium bromide and ammonia/water absorption chillers (Storckenmaier et al., 2003; Safarik et al., 2004).

While absorption cooling has been common for decades, heat pump applications have only in recent years become relevant, due to the improvement in the performance figures; small gas-driven absorption heat pumps achieve coefficients of performance of approximately 1.5, i.e. using 1 kWh of the primary energy of gas, 1.5 kWh of heat can be produced using environmental energy, which is better than the condensing boilers presently available on the market with maximum COP's of about 1.0. Different manufacturers are producing absorption heat pumps with 10 – 40 kW output which achieve COP's of about 1.3 at heating temperatures of 50°C. However, today absorption chillers are mainly used as cooling machines rather than heat pumps.

Absorption cooling machines are categorized either by the number of effects or by the number of lifts: effects refer to the number of times high temperature input heat is used by the absorption machine. In general, increasing the number of effects is meant to increase the COP using higher driving temperature levels. Lifts refer to the number of generator/absorber pairs to successively increase the refrigerant concentration in the solution and to thus reduce the required heat input temperature level.

The most important restrictions of single-effect absorption cooling machines are the limitation of the temperature lifting through the solution field, the fixed coupling of the driving temperature with the temperature of heat source and heat sink and the COP not being larger than 1.0 independent of temperature lifting (Ziegler, 1998). The aim of multistage processes is to overcome these restrictions.

Several types of absorption cooling machines are available on the market: single-effect (SE) and double-effect (DE) ACMs with the working pair water/lithium bromide as well as single-effect (SE) and double-lift (DL) ACMs with the working pair ammonia/water.

The single-effect/double-lift (SE/DL) cycle with the working pair water/lithium bromide is a novel technique. Further cycle designs such as triple-effect (TE) ACM, other multistage cycles and the use of the described cycles for solar cooling have been investigated by a number of researchers (Kimura, 1992; Lamp et al., 1997; Höper, 1999; Ziegler, 1999).

Typical performance characteristics for the closed ACM cycles described above are stated in table

Table 1: Water lithium bromide absorption chiller characteristics.

Cycle type	SE	DE	SE/DL
cold temperature / °C	6 – 20	6 – 20	6 – 20
heating temperature / °C	70 – 110	130 – 160	65 – 100
cooling water temperature / °C	30 – 35	30 – 35	30 – 35
COP / –	0.5 – 0.7	1.1 – 1.3	0.4 – 0.7

Table 2: Performance of NH₃/H₂O absorption chillers and Diffusion-Absorption machines with auxiliary gas.

Cycle type	SE	DL	SE
auxiliary gas	–	–	hydrogen/helium
cold temperature / °C	-30 – 20	-50 – 20	-20 – 20
heating temperature / °C	90 – 160	55 – 65	100 – 140
cooling water temperature / °C	30 – 50	30 – 35	30 – 50
COP / –	0.4 – 0.6	0.4	0.2 – 0.5

1 for water/lithium bromide and in table 2 for ammonia/water.

History of solar cooling with absorption chillers

In the 1970th, the company Arkla Industries Inc., USA (now owned by Robur SpA, Italy), developed the first commercial, indirectly driven, single-effect H₂O/LiBr ACM for solar cooling with two different nominal cooling capacities. The driving heat temperatures were in the range of 90°C and the cooling water temperature was 29°C for 7°C cold water temperature. The machine was installed in demonstration projects more than 100 times in the USA (Loewer, 1978; Lamp et al., 1997; Grossmann, 2002). Arkla and also Carrier Corp., USA, then developed a small size single-effect H₂O/LiBr ACM that could work with air cooling. There was no market success mainly due to the high investment costs for solar cooling. Carrier Corp. further decreased the driving temperature of a water-cooled single-effect H₂O/LiBr ACM by using a falling film generator with a large surface area. The driving heat temperature was 82°C and the cooling water temperature was 28°C for 7°C cold water temperature (Lamp et al., 1997). The production of these ACMs was stopped and the technology's licence was given to the Japanese company Yazaki. Up to the beginning of the 1990th, the company Yazaki offered H₂O/LiBr ACMs with 5 – 10 kW cooling power (such as the WFC-600 with 7 kW), which were used for solar cooling projects. Due to the missing demand, the production was also stopped.

At the beginning of the 1980th, Arkla developed a double-effect H₂O/LiBr ACM in which the lower temperature generator was supplied with solar energy, while in fossil mode the double-effect generator

was fired using the higher COP. Due to the lack of demand on the market for solar cooling, the production of this cooling machine was stopped and the technology was also licensed to the Japanese company Yazaki. They sold the machines for several years, but they are no longer available today.

In the medium-sized performance range, the most project experiences for solar cooling exist for the single-effect water/lithium bromide ACM WFC-10 from Yazaki, Japan, with a cooling power range of 35 – 46 kW. The operation is generally rated as dependable and unproblematic.

After the market failure of low power systems some decades ago, there has been an increased interest in low power absorption chillers during the last decade. A range of manufacturers - many from Europe - now offer single effect thermal chillers with cooling power below 10 kW. The Swedish company ClimateWell alone installed several hundred units in Spain during the last two years, while in 2007 the total number of solar cooling systems was estimated at only 200 (Preisler, 2008: Case study Rococo, Arsenal Research).

There are no general rules yet for the dimensioning of solar cooling systems and planners often do not have adequate tools to determine the energy yield and solar fraction. The ratios between solar collector surface area and cooling power or storage volume and collector surface in the various demonstration projects vary strongly (see figure 1). Under comparable climatic conditions - Austria and Germany, for example - less than one and more than five square meters of collectors have been installed per kilowatt of cooling power.

Also the ratio of storage volume (in liter water volume) to installed collector surface varies by more than a factor 20 in the different demonstration projects. While warm water solar thermal systems or heating support systems have typical storage volumes between 50 and 100 liter per square meter of collector surface, in the solar cooling projects storage volumes are often much lower with less than 30 liter per square meter of collector. However, there are also some projects with significant storage volumes over 100 liter per square meter (see figure 2).

The ratio of installed collector surface to the cooled building surface spreads over a wide range of values from under 10% up to 30% of the building surface area (see figure 3). It is clear that the solar contribution to the total cooling demand must vary significantly. Unfortunately very few published results of measured solar fractions are available today.

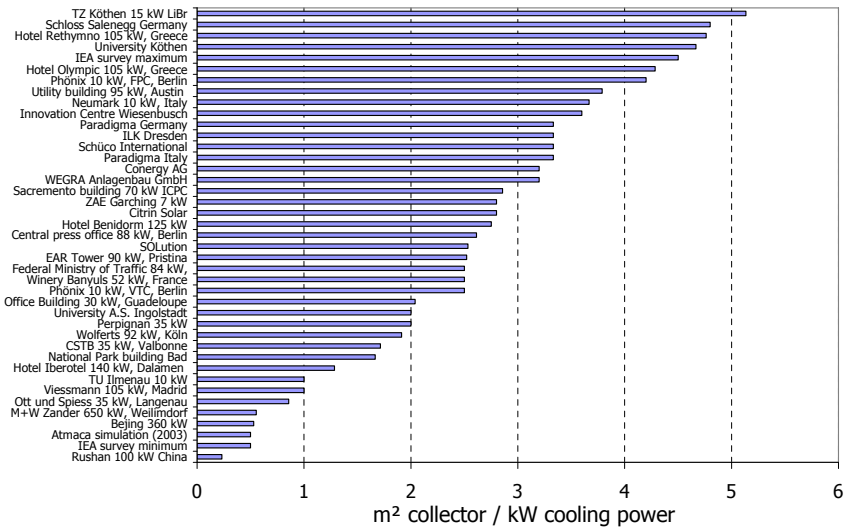


Figure 1: Collector surface per kW of cooling power in various demonstration projects.

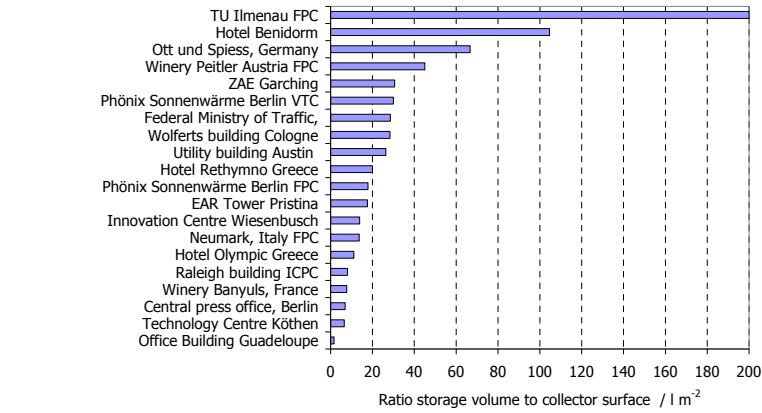


Figure 2: Ratio of hot water storage volume in liter per square meter of collector surface for different solar cooling demonstration projects.

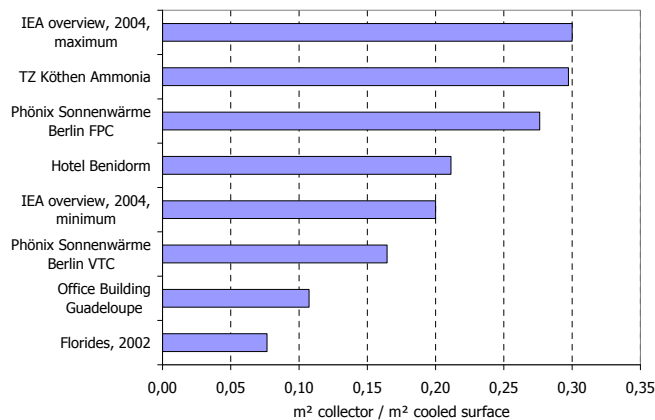


Figure 3: Ratio of installed collector surface area to building surface area in various demonstration projects.

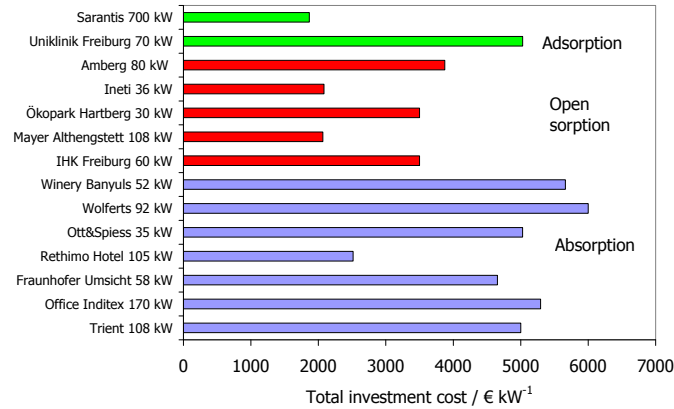


Figure 4: Total investment costs for different solar cooling systems implemented in the last decades in Europe.

For some of the solar cooling systems described above, total investment costs are available. Depending on system size and technology chosen, the total investment cost vary between 1900 and 6000 € per kilowatt cooling power installed (see figure 4).

Design, performance and optimisation potentials of solar driven absorption cooling systems

Dynamic simulation showed that the design and dimensioning of a solar thermal system for cooling applications depends not just on the maximum cooling load, but on the characteristics of the cooling load distribution over the year (Assilzadeh et al, 2004; Mittal et al, 2005; Eicker et al, 2007; Bujedo et al, 2008). On the plant side the overall performance of the ACM is significantly influenced by the control of the cooling temperature at absorber and condenser inlet, the required cold water temperature and the heating temperature on the generator side. The solar fraction of the required heating energy depends not just on the collector and hot storage size, but also on the specific mass flow rate of the collector field, the control of the collector pump and the charge and discharge control of the hot storage. In the following these influencing factors on the performance of solar driven absorption chillers are discussed separately, starting with the influence of the building and its cooling load characteristics and locations and then dealing with the influence of the control of the solar system.

Influence of the building and location on the design and performance of solar driven ACM

For the dimensioning of the solar cooling system information about the maximum cooling load of the building is required to choose the correct size of the absorption chiller, but is not sufficient for the dimensioning of the solar system to achieve a certain solar fraction. The main reason for this is that different buildings have different daily cooling load characteristics with the maximum cooling power required earlier or later during day and the problem of a fixed timely availability of solar energy. To overcome these shifts between maximum cooling load and maximum solar irradiation or cloudy days with low solar irradiation, hot or cold water storage tanks can be introduced into the system. Another problem results from the fact that the available solar energy not only depends on the time of the day but also on the time of the year and that the cooling load of some buildings is not that closely related to the ambient conditions as others are. For example the cooling load of buildings with medium to low internal loads and large window areas is typically much closer linked to the available solar irradiation than buildings with low window areas or good shading protection but much higher internal loads. To reach the same solar fraction the second type of building needs much larger collector fields and hot water storage tanks although both building types may have the same maximum cooling load.

The location has a clear influence on the required cooling load of the buildings but also has a distinctive influence on the performance of the solar cooling system. Apart from the available solar irradiation the most critical parameters for the efficiency of the absorption cooling system are the ambient temperature and humidity. These two values strongly influence the cooling water temperature of the absorber and condenser which has a significant influence on the performance of the absorption chiller. However, so far very few results of complete system simulations and even less measured performance data have been published.

Different building types were compared by Henning for a range of climatic conditions in Europe with cooling energy demands between 10 and 100 kWh m⁻²a⁻¹. Collector surfaces between 0.2 and 0.3 m² per square meter of conditioned building space combined with 1–2 kWh of storage energy gave solar fractions above 70% (Henning 20004). System simulations for an 11 kW absorption chiller using the dynamic simulation tool TRNSYS gave an optimum collector surface of only 15 m² for a building with 196 m² useful floor area and 90 kWh m⁻² annual cooling load, i.e. less than 0.1 m² per square

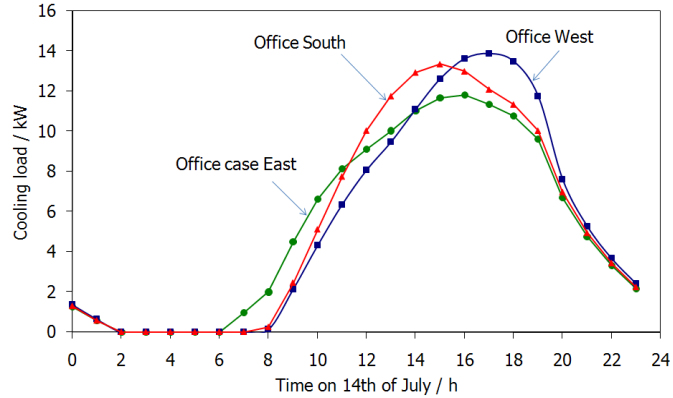


Figure 5: Hourly cooling loads for an office building with low internal loads with its main window front facing in different directions.

meter of useful building floor area. A storage volume of 0.6 m^3 was found to be optimum (40 l/m^2 collector), which at 20 K useful temperature level only corresponds to 14 kWh or 0.07 kWh per square meter of useful building floor area (Florides, 2002). Another system simulation study (Atmaca, 2003) considered a constant cooling load of 10.5 kW and a collector field of 50 m^2 . 75 l storage volume per square meter of collector surface were found to be optimum. Larger storage volumes were detrimental to performance. Also attempts have been made to relate the installed collector surface to the installed nominal cooling power of the chillers in real project installations. The surface areas varied between 0.5 and $5 \text{ m}^2\text{kW}^{-1}$ of cooling power with an average of $2.5 \text{ m}^2\text{kW}^{-1}$.

A recent simulation study discussed the influence of building loads on solar thermal system dimensioning (Eicker et al, 2008). Here the orientation, location and internal loads of the building were varied. The peak values of the daily cooling loads are highest for an office with a large western window front and lowest for an office with the main windows orientated to the east (see figure 5). The phase shift between the maxima of the curves is about 2h with the maximum of the eastern and south orientated buildings at around 3pm and of the west orientated building at around 5pm , which demonstrates the typical phase shift between the maximum solar radiation (1pm at summer time) and the cooling load of buildings. A wide range of specific cooling energies is covered, ranging from about 10 kWh m^{-2} for an office with low internal loads in a moderate climate up to 70 kWh m^{-2} for the same building in Madrid and high internal loads.

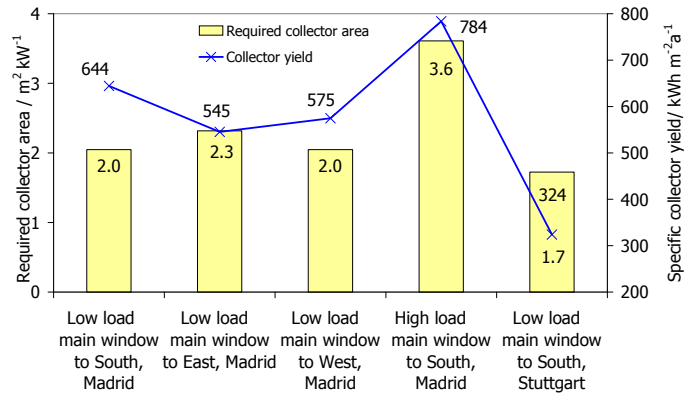


Figure 6: Required collector area for 80% solar fraction per max. cooling load and resulting collector yield

If a given cooling machine designed to cover the maximum load is used for different building cooling load profiles, the influence of the specific load distribution and annual cooling energy demand can be clearly seen (see figure 6). An office building with low internal loads and the main windows facing south requires about $2 \text{ m}^2\text{kW}^{-1}$ solar thermal collector area for a solar fraction of 80% at the location Madrid. If the building orientation is changed, the peak cooling power also changes. To adjust for these differences the building surfaces areas were adapted to give the same maximum cooling load. The different orientations then change the required collector area by about 10-15%.

More significant is the impact of the building internal loads, which strongly increases the full load hours for a given cooling peak power. Here the required collector surface area is nearly double with $3.6 \text{ m}^2\text{kW}^{-1}$, although the required maximum power is still the same. Due to the longer operating hours of the solar thermal cooling system, the specific collector yield is 20% higher and a mean solar thermal system efficiency of 45% can be obtained for solar cooling operation alone. If the office building with low internal loads is placed in Stuttgart/Germany with a more moderate climate, the collector yield drops by 60% to about $300 \text{ kWh m}^{-2}\text{a}^{-1}$.

The storage volumes are comparable to typical solar thermal systems for warm water production and heating support (between 40 and 100 l/m^2 of collector aperture area, depending on the cooling load file). They increase with cooling energy demand for a given location. In moderate climates with only occasional cooling energy demand, the storage volumes are generally higher.

For the location Madrid, the collector surface area required to cover 1 MWh of cooling energy

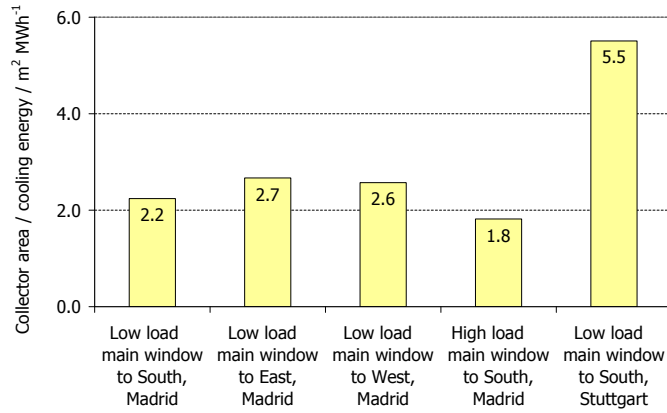


Figure 7: Required collector area for 80% solar fraction related to the annual cooling energy demand demand is between 1.8 and 2.7 m² per MWh, depending on building orientation chosen. The lower the cooling energy demand, the higher the required collector aperture area per MWh. This is very clear for the building in Stuttgart with a low total energy demand of about 10 kWh m⁻² a⁻¹, where 5.5 m² solar thermal collector aperture area per MWh is necessary to cover the energy demand (see figure 7).

The work shows that dynamic system simulations of the building and solar cooling system so far are the only reliable possibility to determine the correct solar thermal system size to reach a certain solar fraction of the total energy requirement.

Influence of system configuration and control strategy

Apart from the cooling load characteristic of the buildings the design and performance of solar driven absorption cooling systems depend on the chosen system configuration and control including the chillers, the cooling tower, the installed cooling distribution system and the solar heating system (Henning, 2004; Sumath, 2003; Kohlenbach, 2007). A cold distribution with high cold water temperatures, i.e. in case of chilled suspended ceilings or thermally activated concrete structures, allows the absorption chiller to work on a much higher COP. Less collector area is therefore required to achieve the same solar fraction than in case of air based distribution systems with low cold water temperatures. The decision for a wet or dry cooling tower/recooler has a similar but even more significant effect on the required collector area since the cooling water temperature strongly influences the thermal COP of the absorption chiller. Some of the installed systems operate at constant high generator temperature

Table 3: Analysed system configurations and control options for a low internal load building.

Analysed cases	control options					
	Cooling tower		cold distribution temperature		Generator inlet temperature	
	Type	Set point cooling water	6°C / 12°C	15°C / 21°C	85°C constant	70-95°C variable
Case 1	wet	27	x		x	
Case 2	wet	27	x			x
Case 3	wet	27		x		x
Case 4	dry	27		x		x

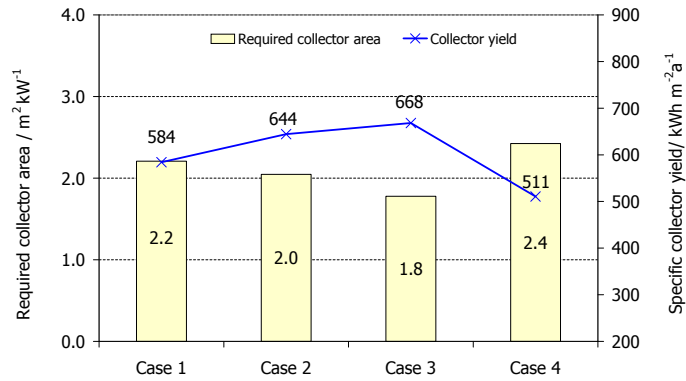


Figure 8: Required collector area related to max cooling load and resulting collector yield for 80% solar fraction (Office building in Madrid, Spain with low internal loads)

which results in a slightly higher thermal COP but lower solar fractions compared to systems where the generator inlet temperature is allowed to vary according to the temperature level available in the hot storage tank. Different control options are summarized in table 3 and the results of the analysed cases are shown in figures 8 and 9. If a wet cooling tower is used, the required collector surface area can be reduced by about 20% to 1.8 m² per kW, if the cold water temperature level is high and a variable generator inlet temperature is used (Case 3). If dry recooling is used at the same cold water and generator temperature levels, this leads to 33% more collector surface area (2.4 m² per kW cooling power). In addition the solar thermal system efficiency is highest at nearly 40% for high cold water temperature levels and variable generator inlet temperatures.

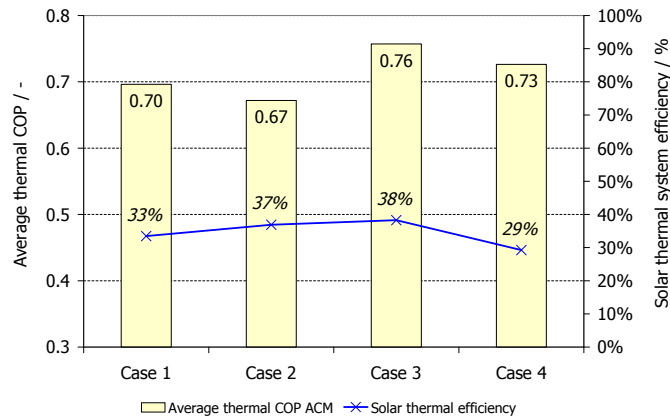


Figure 9: Average annual COP and solar thermal system efficiency for different system configurations and control strategies

Auxiliary energy consumption

High electricity consumption caused by inefficient pumps, bad hydraulic design and suboptimal control in combination with low solar fractions through insufficient system design are critical for the environmental and economical performance of installed absorption cooling systems, especially if they are compared to highly efficient electrical driven compression chillers (Kohlenbach, 2007). Most of the recent publications on the performance of solar cooling systems are focusing on the thermal COP and the solar fraction reached. The electricity consumption of the absorption chiller, the cooling tower and all pumps are not discussed in detail. However, since this technology is now more and more leaving the prototype and demonstration status towards a proven technology which needs to compete with highly efficient electrical compression chillers the awareness of the importance of this issue is increasing significantly. Within TASK 38 therefore standardised monitoring requirements are currently developed to overcome the problem of missing electricity and heat meters in demonstration installations. In parallel these monitoring guidelines are applied to a large number of demonstration installations to get reliable monitoring data of existing systems, which are not yet available.

To demonstrate the effect of different control strategies on the overall performance of solar driven absorption chillers the results of a recent study (Pietruschka et al, 2007) on the performance of a solar driven absorption cooling system installed in an office building in Rimsting, Germany are discussed. This system includes a market available 15 kW LiBr absorption chiller, two 1 m³ hot water storage

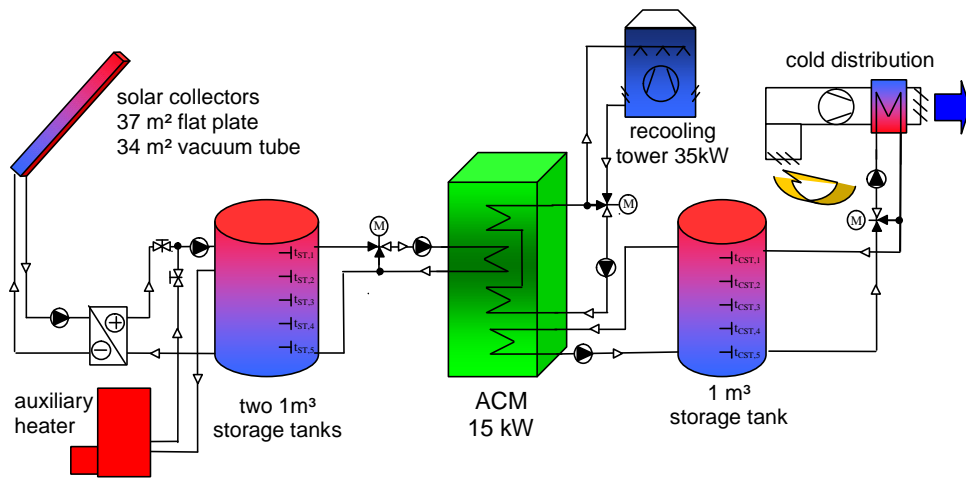


Figure 10: Schematic drawing of a solar driven absorption cooling system used for control strategy optimisation.

tanks, one 1 m³ cold storage tank, 37 m² flat plate collectors and 34 m² solar vacuum tube collectors all facing south with an inclination of 30°, a 35 kW wet recooling tower and an additional dry recooling system (see figure 10). For the distribution of the cooling energy chilled ceilings and fan coils are used with 16°C supply and 18°C return temperature and an automated supply temperature increase for dew point protection. The office building with 566 m² of conditioned space has a maximum cooling load of 18 kW and a total annual cooling energy demand of 8.7 MWh/a (16 kWh/m²a).

The installed absorption chiller is able to provide the required cooling power of 18 kW if the setpoint of the recooling temperature is reduced by 3 K from 30°C design conditions to 27°C. For the analysis of different control strategies on the overall performance of the installed system a detailed dynamic simulation model developed in INSEL (Schumacher, 1991) was used which also considers the electricity consumption of all installed components (fans, pumps, etc.). Five main cases with different control options have been analysed (see table 4). Three of them operate with wet cooling towers, case 4 and 5 with dry recooling.

The setpoint of the recooling water temperature is either controlled by a 3-way-valve or by fan speed control of the cooling tower. Values below 27°C (30°C for dry cooling tower) are only provided as long as reachable at the given ambient conditions with the chosen recooling technologie. The Generator inlet temperature is either constant or variable according to the temperature in the hot and cold storage tank.

Table 4: Analysed control options of the absorption cooling system.

Analysed cases		Case 1	Case 2	Case 3	Case 3.1	Case 3.2	Case 4	Case 5
Cooling tower	type	wet	wet	wet	wet	wet	dry	dry
Cooling water temp. control	3-way-valve	x					x	
	fan speed		x	x	x	x		x
Cooling water setpoint	27°C	x	x	x			x	x
	24°C				x			
	21°C		x			x		
Generator temperature setpoint	90°C	x	x					
	70-90°C			x	x	x		
	70-95°C						x	x
Control dist. pump ΔT -control	yes		x	x	x	x	x	x
	no	x						

An additional Case 6 is defined and analysed as reference system for a compression chiller using manufacturer's data with an electrical COP of 4.0 at 27°C recooling temperature. The recooling is done with a dry recoler with constant fan speed control, which tries to keep the 27°C if possible.

For a detailed analysis of the system performance annual simulations were carried out for the regarded cases with different control options as defined in table 4 and for the reference compression chiller system of Case 6. The main results are summarised in three graphs shown in figures 11 to 13. To compare the efficiency of the system with varied control strategies three different COP are used: 1. The standard thermal COP_{th} which is defined as the cooling energy produced divided by the heating energy used; 2. The total electrical COP_{el} which is simply the cooling energy produced divided by the total electricity consumption of the solar cooling system; 3. The total primary energy (PE) related COP which is defined as the provided cooling power divided by the sum of consumed electricity and auxiliary thermal energy multiplied by the PE factors of 3.0 for electricity and 1.1 for the gas boiler.

$$COP_{PE,total} = Q_{cool} / (3Q_{el} + 1.1Q_{h,aux}) \quad (1)$$

The average thermal COP is in most cases around 0.74 and can be slightly increased to 0.77 by reducing the recooling temperature setpoint (Figure 11). Therefore the required heating energy is nearly constant for all analysed cases at a value of slightly below 650 kWh per kW maximum cooling load. A more significant influence of the different control strategies is visible for the solar fraction

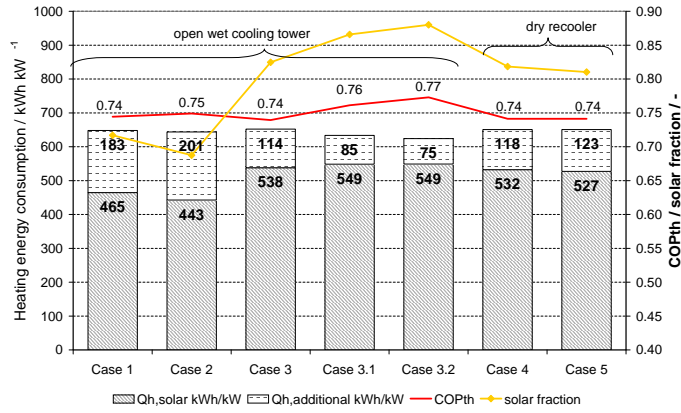


Figure 11: Comparison of heating energy consumption related to maximum cooling load, COPth and solar fraction

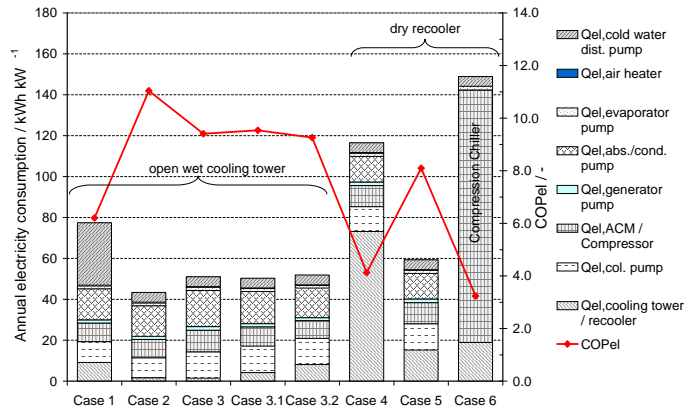


Figure 12: Comparison of electricity consumption related to max. cooling load and electrical COP for different control strategies and system temperatures.

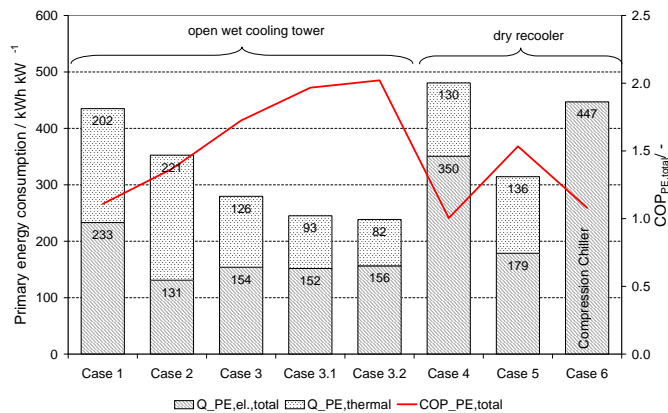


Figure 13: Comparison of primary energy consumption related to maximum cooling power and primary energy based COP

reached. Cases with constant generator inlet temperature reach the lowest solar fractions of around 70%. If the generator inlet temperature is allowed to vary according to the temperature in the hot storage tank and the required cooling load this value can be increased up to 88% for the case with the lowest recooling temperature setpoint.

The electricity consumption strongly depends on the fact whether the cold water distribution pump of the building and the ventilator of the cooling tower are controlled according to the load or not. For the absorption cooling system the electricity consumption related to the maximum cooling load varies between 42 and 120 kWh kW⁻¹ with the highest value for systems with dry coolers without fan speed control (Figure 12). The electricity consumption of these systems is quite close to the electricity consumption of a system with compression chiller which consumes 150 kWh kW⁻¹. Highly efficient systems with controlled distribution pump and wet cooling towers with fan speed control consume only 50 kWh kW⁻¹ which is one third of the system with compression chiller. The electrical COPs vary between 6.5 and 11 for the cases with wet cooling tower and between 4.2 and 8 for the cases with dry cooling tower. The compression chiller reaches an overall electrical COP of 3.6 which is only slightly below the worst absorption cooling system.

If the primary energy related COP and the primary energy consumption is analysed (Figure 13), it becomes obvious that badly controlled absorption cooling systems do not save any primary energy compared to compression chillers. Only systems with highly efficient pumps, cooling towers with fan speed control and ΔT -mass flow control of the cold distribution pump are able to significantly save primary energy. The primary energy related COP of these systems is between 1.5 and 2 which means that in the best case nearly half of the primary energy consumption of a system with compression chiller can be saved with well designed and controlled solar cooling systems.

To avoid additional heating energy consumption and to increase the primary energy savings some systems are designed for purely solar driven operation. However, these systems are either designed with very large collector areas and huge hot storage volumes or an auxiliary electrical cooling system has to be used. To start the operation of absorption chillers a certain temperature level needs to be available either in the hot storage tank or in the collector circuit in case of direct solar driven systems without hot storage tank. Large hot water storage tanks require time to be heated up in the morning, therefore

such systems suffer from a late start-up of the absorption chiller in the morning. Direct solar driven systems without hot water storage only need to heat up the collector circuit and therefore can start the absorption chiller operation much earlier. On the other hand, these systems often have the problem of unstable operation of the absorption chiller on cloudy days caused by system shut downs and start-ups due to insufficient heat supply. To combine the advantages of both systems the hot storage tank can either be partitioned in a smaller upper part and a bigger lower part or bypassed completely. Both possibilities require the implementation of intelligent storage charge and discharge control strategies. In a recent study (Pietruschka et al, 2008) the solar cooling system described above was considered to be purely solar driven and analysed for different storage charge and discharge strategies. The results show, that through the implementation of a storage bypass the start-up time can be significantly reduced by 1h 40 min in the worst and nearly 2 h in the best case. For the partitioned storage case (300 liter top and 1700 liter bottom volume), the start-up time is between 12 and 20 minutes later. On a cloudless summer day the start-up of the solar cooling system is at 9:23am (Bypass), 9:43am (partitioned storage) instead of 11:04am (full storage). The overall best performance is reached for a system with combined bypass and partitioned storage control with system start-up at 9:23am and stable system operation on cloudy days. Compared to a system which always uses the full storage volume the combined system with partitioned storage and storage bypass can produce between 19 % (cloudless days) and 33% (cloudy days) more cooling energy per day.

Technology overview: desiccant cooling

Desiccant cooling systems are an interesting technology for sustainable building climatisation, as the main required energy is low temperature heat, which can be supplied by solar thermal energy or waste heat. Desiccant processes in ventilation mode use fresh air only, which is dried, precooled and humidified to provide inlet air at temperature levels between 16 – 19°C. The complete process is shown in figure 14 with the fresh air side and the exhaust air side. Outside air (1) is dried in the sorption wheel (2), precooled in the heat recovery device with the additionally humidified cool space exhaust air (3) and afterwards brought to the desired supply air status by evaporative cooling (4). The space exhaust air (5) is maximally humidified by evaporative cooling (6) and warmed in the heat

recovery device by the dry supply air (7). In the regeneration air heater the exhaust air is brought to the necessary regeneration temperature (8), takes up the water adsorbed on the supply-air side in the sorption wheel, and is expelled as warm, humid exhaust air (9). If room air is recirculated, the desiccant wheel is used to dry the room exhaust air, which is then precooled using the rotating heat exchanger and humidified to provide the cooling effect. Regeneration of the desiccant wheel and precooling of the dried recirculation air is done by ambient air, which is first humidified, then passes the rotating heat exchanger, is heated to the necessary regeneration temperature and finally used to regenerate the desiccant wheel.

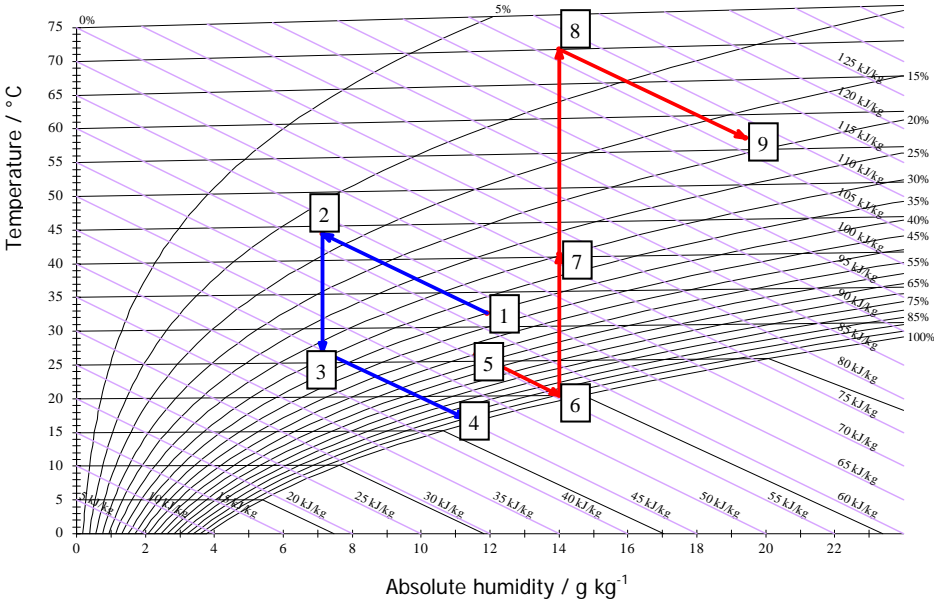


Figure 14: Process steps of a desiccant cooling system in a hx-diagram.

The concept of desiccant cooling was developed in the 1930th and early attempts to commercialize the system were carried out unsuccessfully. Pennington patented the first desiccant cooling cycle (Pennington, 1955), which was then improved by Carl Munters in the 1960th (Munters, 1960). Good technology overviews are given by Mei, Lavan and others (1992) or Davanagere et al (1999). The most widely used desiccants are silica gel, lithium chloride or molecular sieves, for example zeolites. Solid desiccants such as silica gel adsorb water in its highly porous structure. Lithium chloride solution is used to impregnate for example a cellulose matrix or simpler cloth based constructions and can then be used to absorb water vapour from the air stream (Hamed et al, 2005).

The thermal coefficient of performance is defined by the cold produced divided by the regeneration heat required. For the hygienically needed fresh air supply the enthalpy difference between ambient air and room supply air can be considered as useful cooling energy. If the building has higher cooling loads than can be covered by the required fresh air supply, then the useful cooling energy has to be calculated from the enthalpy difference between room exhaust and supply air, which is mostly lower. The thermal COP is obtained from the ratio of enthalpy differences (state points are given in brackets):

$$COP_{thermal} = \frac{q_{cool}}{q_{heat}} = \frac{h_{amb(1)} - h_{supply(4)}}{h_{waste(9)} - h_{reg(8)}} \quad (2)$$

Related to ambient air, COP's can be near to 1.0, if regeneration temperatures are kept low and reduces to 0.5, if the ambient air has to be significantly dehumidified. COP's obtained from room exhaust to supply air are lower between 0.35 and 0.55 (Eicker, 2003). The maximum COP of any heat driven cooling cycle is given for a process, in which the heat is transferred to a Carnot engine and the work output from the Carnot engine is supplied to a Carnot refrigerator. For driving temperatures of 70°C, ambient air temperatures of 32°C and room temperatures of 26°C, the Carnot COP is 5.5.

$$COP_{Carnot} = \left(1 - \frac{T_{ambient}}{T_{heat}}\right) \left(\frac{T_{room}}{T_{amb} - T_{room}}\right) \quad (3)$$

However, as the desiccant cycle is an open cycle with mass transfer of air and water, several authors suggested to rather use a reversible COP as the upper limit of the desiccant cycle, which is calculated from Carnot temperatures given by the enthalpy differences divided by entropy differences (Lavan et al, 1982). This allows the calculation of equivalent temperatures for the heat source (before (7) and after the regenerator heater (8)), evaporator (room exhaust (6) minus supply (4)) and condenser (Waste air (9) minus ambient(1)).

$$T_{equivalent} = \frac{\sum m_{in} h_{in} - \sum m_{out} h_{out}}{\sum m_{in} s_{in} - \sum m_{out} s_{out}} \quad (4)$$

Under conditions of 35°C ambient air temperature and 40% relative humidity, defined by the American Air conditioning and Refrigeration Institute (so called ARI conditions), reversible COP's of 2.6 and 3.0 were calculated for ventilation and recirculation mode (Kanoglu, 2007). The real process,

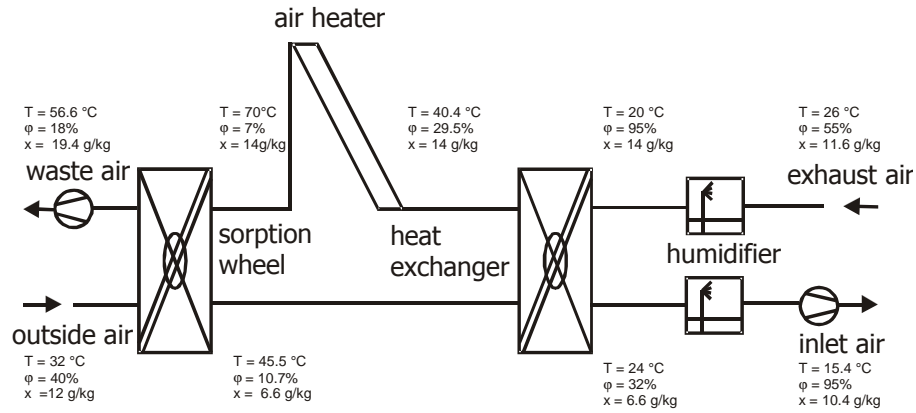


Figure 15: Temperature and humidity levels in a high performance desiccant cooling process.

however, has highly irreversible features such as adiabatic humidification. Furthermore, the specific heat capacity of the desiccant rotor increases the heat input required.

An effective heat exchange is crucial for the process between the dried fresh air (state 2) and the humidified exhaust air (state 6), as the outside air is dried at best in an isenthalpic process and is warmed up by the heat of adsorption. For a rather high heat exchanger efficiency of 85%, high humidification efficiencies of 95% and a dehumidification efficiency of 80%, the inlet air can be cooled from design condition of 32°C and 40% relative humidity to below 16°C (see figure 15).

Simple models have been used to estimate the working range of desiccant cooling systems, for example to provide room conditions not just for one set point, but for a range of acceptable comfort conditions (Panaras et al., 2007). The performance of the desiccant rotor itself can be evaluated by complex heat and mass transfer models based on Navier Stokes equations (Maclaine-Cross, 1988, Gao et al, 2005). This allows the evaluation of the influence of flow channel geometry, sorption material thickness, heat capacity, rotational speed, fluid velocity etc. They are mostly too time consuming to be used in full system simulations including solar thermal collectors, where mostly simpler models are available, based either on empirical fits to measured data (Beccali et al., 2003) or on models of dehumidification efficiency.

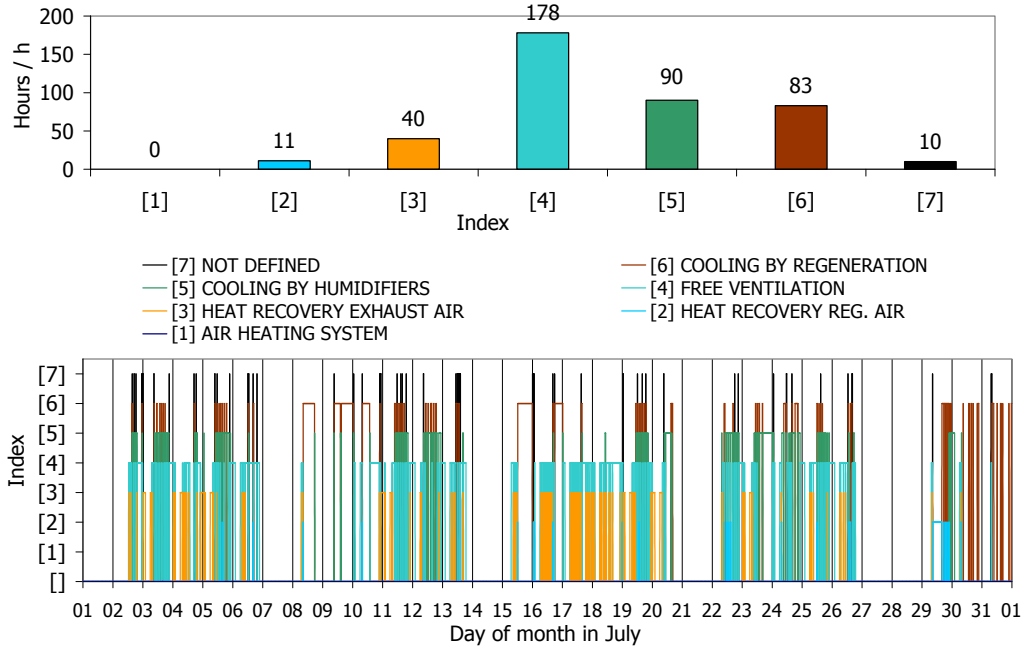


Figure 16: Operation hours of different DEC modes for all days in July for the system of the Maier factory Althengstett in Germany.

Operating experiences desiccant cooling

There are only a few desiccant plants implemented which are powered by solar energy so that operational experience from such plants is very scarce. A common conclusion from three systems in Germany and Spain (IHK building in Freiburg/Germany, Factory Maier in Althengstett/Germany and Public Library Mataró/Spain) driven by solar air collectors was that the solar collector yield during the summer period was below $100 \text{ kWh m}^{-2} \text{ a}^{-1}$ and thus rather low. This is not due to the efficiency of the solar air collectors, which is quite high around 50% for temperature levels of 70°C , but rather to the low numbers of hours during which regeneration is really needed: if the ambient air is not very humid and temperature levels moderate, the pure evaporative cooling effect is sufficient to cool the ambient air. A detailed analysis of the Maier factory building in Germany showed that from 421 operation hours of the system in the month of July, only 83 hours needed full regeneration mode, while during 90 hours pure evaporative cooling was sufficient. The dominant operation mode even in July was free cooling with 178 operating hours (see figure 16).

From the 83 hours of required regeneration, the collector provided energy during 53 hours, i.e. during 64% of the time and produced a total of $11 \text{ kWh m}^{-2} \text{ month}^{-1}$, which is about the same

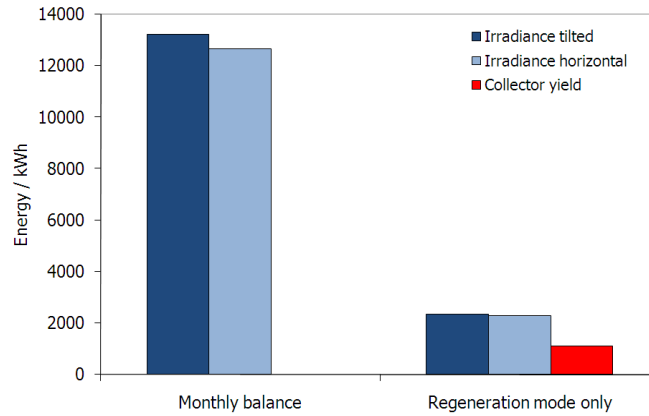


Figure 17: Measured irradiance on collector surface and horizontal plane during July and energy yield during regeneration hours only in the Maier factory building.

amount than the waste heat delivered from the factory machinery. The mean collector efficiency during the operation hours is 48%, which is a good performance value (see figure 17).

Component and control strategy analysis

To reach the design supply air temperatures in desiccant cooling plants, the component performance must be excellent. Measurements in two demonstration plants in Althengstett/Germany and Mataró/Spain showed that heat recovery efficiencies of rotating heat exchangers were only between 62 and 68% at rotation rates of 600 turns per hour. At a measured mass flow ratio between supply and exhaust air of 1.16 the manufacturer value given was 73%. As this component is crucial for the precooling of dried process air, better heat recovery efficiencies should be achieved.

The simple contact evaporators reach 85-86% humidification efficiency, compared to 92% given by the manufacturer. The dehumidification efficiency of sorption rotors, which is defined as the measured absolute dehumidification compared to the maximum possible dehumidification down to the relative humidity of the regeneration air, is 80% at a ratio of regeneration to process air of 66%.

The component parameters from the experimental analysis of the two desiccant cooling units in Spain and Germany are summarised in table 5.

Different control strategies have been compared by Ginestet et al (2003) to study the influence of air volume flow and regeneration temperature. As the increase of regeneration temperature does

Table 5: Summary of measured efficiencies in two desiccant cooling plants in Germany and Spain

	Mataró	Althengstett
Dehumidification efficiency	80	80
Humidification efficiency	86	85
Heat recovery efficiency	68	62

not linearly lower the supply air temperature, the study concluded that increased air flow rates are preferable to increased thermal input, if the cooling demand is high. Mean calculated COP's for the climatic conditions of Nice were between 0.3 and 0.4. Henning and others also remarked that increasing the air flow is useful in desiccant cooling mode, but that the minimum acceptable flow rate should be used in adiabatic cooling or free ventilation mode to reduce electricity consumption (Henning et al, 1999). When thermal collectors with liquid heat carriers are used in combination with a buffer storage, Bourdoukan and others suggested to operate the cooling system only in adiabatic cooling mode during the morning and then allow desiccant operation in the afternoon, using heat from the buffer storage (Bourdoukan et al, 2007). However, in many applications, dehumidification is already required during the morning hours. Also if cheaper air collectors are used, heat storage is not possible.

Desiccant cooling system controllers operate with a temperature cascade system, where usually the exhaust air humidification together with the heat recovery wheel are first switched on, then the supply air humidifier, finally the sorption wheel and if needed the auxiliary energy system. The heat recovery losses from the exhaust air side are avoided if the supply air humidifier is switched on first (for example in the Althengstett project). However, as the room air humidity cannot exceed set values (around 10-12 g/kg), the direct humidification of supply air has limits. The regeneration air temperature has to be limited for certain technologies to avoid damages of the sorption rotor. For example, for cellulose rotor with LiCl solution the maximum allowed regeneration temperature is 72°C.

Each component has specific time delays between the control signal (release) and showing effect in operation. Simple contact humidifiers need about 5 – 10 minutes after release to reduce the air temperature at the outlet significantly and the cooling effect does not stop before 45 minutes after the release is switched off (see figure 18).

This dynamic and partially slow response of the components is often not adequately considered in the control strategy of desiccant cooling plants. For example, supply air temperatures in one of the

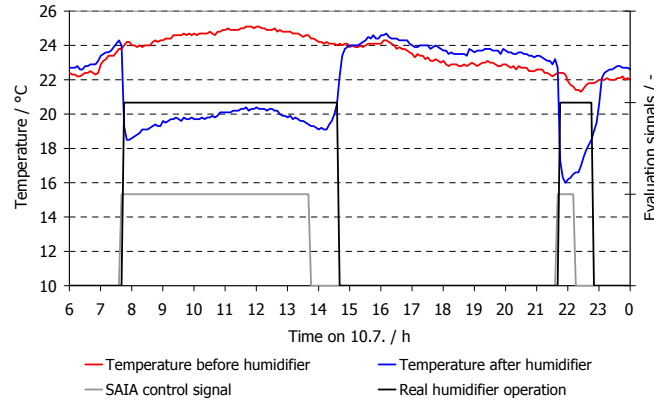


Figure 18: Time delay between control signal and reaction of the humidifier together with signal representing the real operation of the humidifier, when the temperature difference is at least 3 K.

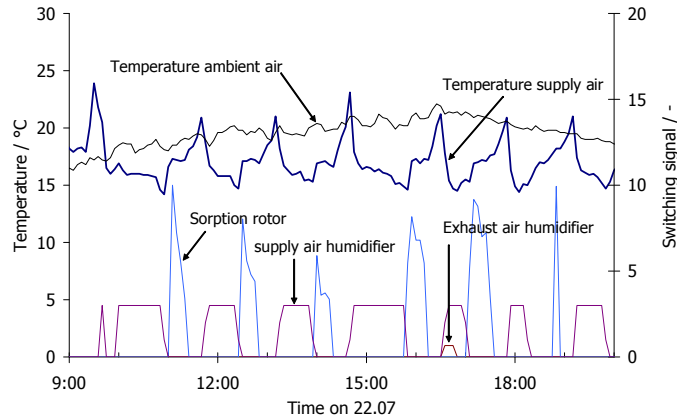


Figure 19: Fluctuations of supply air temperature due to control strategy.

German plants was shown to fluctuate by about 6 K, when supply air humidifiers and heat recovery strategies work against each other. Full humidification of the three stage supply air humidifier leads to a temperature decrease of the supply air below the minimum allowed temperature of 17°C in less than 30 minutes (see figure 19).

The humidifiers are consequently switched off and the rotational speed of the sorption rotor is increased to raise the temperature level in heat recovery mode. Furthermore, the rotating heat exchanger is switched on too early (about 10 minutes before the exhaust air humidifier), so that supply air temperatures increase well above 20°C and then drop again below 15°C. These control problems can be avoided, if the response time of the humidifiers is taken into account and if the sorption wheel is not used in heat recovery mode for compensation of too low temperatures. Furthermore, the rotating

heat exchanger should only switch on together with or five minutes after the exhaust air humidifier.

Fixed high temperature levels for regeneration lead to a high auxiliary energy demand. If temperature setpoints are fixed, auxiliary energy for heating will always be used during the mornings, when solar thermal energy is not yet available at sufficient temperature levels. With air based systems without thermal storage this is difficult to avoid. It is therefore advisable to operate the desiccant mode with low purely solar based regeneration temperatures and admit lower dehumidification rates. Temporary increases of room humidity could then be reduced, when solar energy is available. To use the solar cooling energy also for long operation hours until midnight would only be possible, if the storage mass of the building itself would be used. In conclusion it can be stated that in order to achieve higher solar fractions, the control strategy of the desiccant system must be adapted more to the solar air collector system, allowing full regeneration operation, whenever solar irradiance is available and using the buildings heat and humidity storage capacity to cool and dry it down more than required by static setpoints.

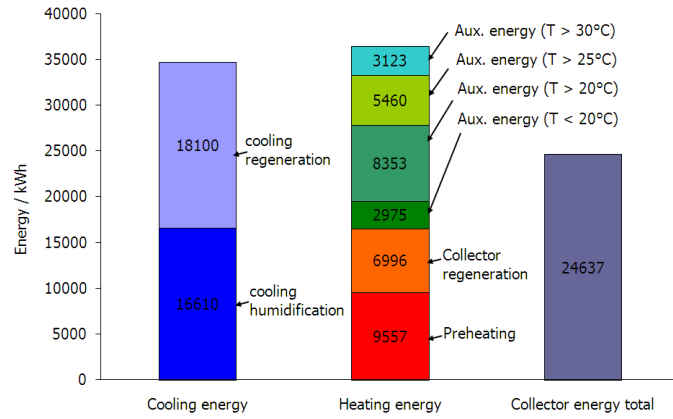


Figure 20: Summer cooling energy produced in the Maier factory building and heating energy for different ambient air temperature ranges. The collector energy is also used for heating of old factory buildings.

Energy analysis and COP's

The coefficient of performance of the desiccant cooling process strongly depends on the ambient boundary conditions: if the dehumidification required is low, the regeneration temperatures can also be low and the COP is high. In case only evaporative cooling is sufficient, the thermal COP is infinite. Typical average COP's over a summer period are near 1.0. If the heating energy is related only to the hours with full desiccant operation, the COP is on average around 0.5. Full desiccant cooling operation is mainly required in the summer months, when the humidification process alone is not sufficient for exterior air cooling. These results were obtained from one year of detailed monitoring results of the Maier factory building (see figure 20).

Under German climatic conditions, about half of the cooling energy is usually obtained with full desiccant operation, the rest of the operating time only humidification is sufficient. An interesting fact is that auxiliary energy is often necessary when outside temperatures are rather low (below 25°C). Although the temperature reduction between outside air and inlet air is small for these condition, the dehumidification process requires a high amount of energy. Auxiliary cooling would be preferable under such conditions. If not possible the controller must ensure that the regeneration air temperature is kept at its minimum and not set to fixed values.

The thermal auxiliary energy demand obviously depends on the dimensions of the solar collector field and the climatic boundary conditions. As regeneration air heating is very energy intensive at

sometimes little cooling effect, it is recommendable to use auxiliary cooling systems. If the electrical COP's are analysed, the additional pressure drops across the humidifiers, sorption wheel and air collector fields have to be considered. Compared to a conventional air conditioning system this means for the Althengstett case about 20% higher electricity consumption. Related to the produced cold, the additional electricity demand corresponds to an average electrical COP of 7.5. If the total electrical energy consumption for an air based distribution system is considered, the ratio of produced cold to total electricity demand is much lower and typically below 2.0. This is a consequence of an air based cooling distribution system. The situation can only be improved if variable volume flows are possible at partial load conditions.

Cost evaluation

To plan and project energy systems such as solar cooling systems, economic considerations form the basis for decision making. The costs in energy economics can be divided in three categories: capital costs, which contain the initial investment including installation, operating costs for maintenance and system operation and the costs for energy and other material inputs into the system.

The analysis presented here is based on the annuity method, where all cash flows connected with the solar cooling installation are converted into a series of annual payments of equal amounts. The annuity a is obtained by first calculating the net present value of all costs occurring at different times during the project, i.e. by discounting all costs to the time $t = 0$, when the investment takes place. The initial investment costs $P(t = 0)$ as well as further investments for component exchange in further years $P(t)$ result in a capital value CV of the investment, which is calculated using the inflation rate f and the discount or basic interest rate d .

$$CV = \sum P(t) \frac{(1+f)^t}{(1+d)^t} \quad (5)$$

Annual expenses for maintenance and plant operation EX , which occur regularly during the lifetime N of the plant, are discounted to the present value by multiplication of the expenses with the present value factor PVF . The system lifetime was set to 15 years.

$$PVF(N, f, d) = \frac{1+f}{d-f} \left(1 - \left(\frac{1+f}{d-f} \right)^N \right) \quad (6)$$

In the case of solar cooling plants, no annual income is generated, so that the net present value NPV is simply obtained from the sum of discounted investment costs CV and the discounted annual expenses. It is here defined with a positive sign to obtain positive annuity values.

$$NPV = CV + EX \times PVF(N, f, d) \quad (7)$$

Annual expenses include the maintenance costs and the operating energy and water costs. For maintenance costs, some standards like VDI 2067 use 2% of the investment costs. Some chiller manufacturers calculate maintenance contracts with 1% of the investment costs. For large absorption chillers, some companies offer constant cost maintenance and repair contracts: the costs vary between 0.5% for large machines (up to 700 kW) up to 3% for smaller power. Repair contracts are even more expensive with 2% for larger machines up to 12% for a 100 kW machine. In the calculations shown here, 2% maintenance costs are used.

To obtain the annuity a as the annually occurring costs, the NPV is multiplied by a recovery factor r_f , which is calculated from a given discount rate d and the lifetime of the plant N . The cost per kWh of cold is the ratio of the annuity divided by the annual cooling energy produced.

$$a = NPV \times r_f(N, d) = NPV \times \frac{d(1+d)^N}{(1+d)^N - 1} \quad (8)$$

Cost and economics of absorption chillers

An own market study gives an overview of the investment costs for the chillers (see figure 21). In addition to the chiller investment costs, the annuity of the solar thermal system depends on the surface area of the collector field, the storage costs and the costs for system integration and mounting. Cost information for the solar thermal collectors and storage volumes were obtained from a German database for small collector systems, from the German funding program Solarthermie 2000 for flat plate collector surface areas above 100 m² and for vacuum tube collectors from different German distributors

(see figure 22 and 23).

Maintenance costs and the operating costs for electrical pumps were set to 2%. Major unknowns are the system integration and installation costs, which depend a lot on the building situation, the connection to the auxiliary heating or cooling system, the type of cooling distribution system and so on. Due to the small number of installations, it is difficult to obtain reliable information about installation and system integration costs. Two prices were there calculated: the first with very low installation costs of 5% of total investment plus 12% for system integration. A second price is based on 25% installation and 20% system integration costs.

The total costs per MWh of cold produced C_{total} are obtained by summing the chiller cost $C_{chiller}$ to the solar costs C_{solar} , the auxiliary heating costs C_{aux} and the costs for the cooling water production $C_{cooling}$. The costs for heating have to be divided by the average COP of the system to relate the cost per MWh heat to the cold production and multiplied by the solar fraction s_f for the respective contributions of solar and auxiliary heating. For the cooling water, the costs per MWh of cooling water were taken from literature (Gassel, 2004) and referred to the MWh of cold by multiplication with $(1 + \frac{1}{COP})$ for removing the evaporator heat (factor 1) and the generator heat with a factor $\frac{1}{COP}$.

$$C_{total} = C_{chiller} + \frac{s_f C_{solar}}{COP} + \frac{(1 - s_f) C_{aux}}{COP} + C_{cooling} \left(1 + \frac{1}{COP}\right) \quad (9)$$

A value for $C_{cooling}$ of 9 € per MWh cooling water was used and the auxiliary heating costs $C_{heating}$ were set to 50 € per MWh of auxiliary heat.

The chosen system technology (dry or wet chiller, low or high temperature distribution system, control strategy) influences the costs only slightly (7% difference between the options), if the operating hours are low (see figure 25). If the operating hours increase, the advantage of improving the control strategy or increasing the temperature levels of the cooling distribution system become more pronounced (16% difference between the different cases, see figure 26).

For very low operating hours such as an office building in the Stuttgart climate with low internal loads (only about 300 full load hours), the costs are between 790 and 860 € MWh⁻¹, 60% of which are due to the chiller investment costs only (see figure 24).

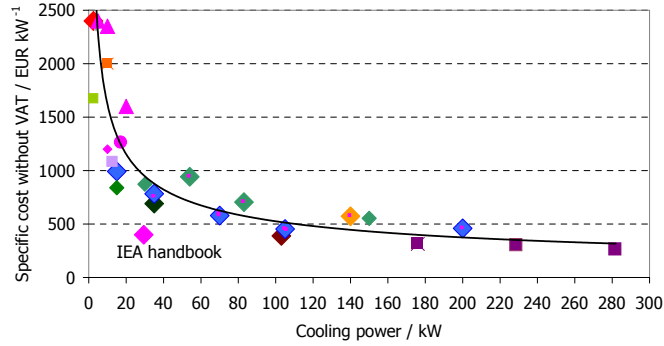


Figure 21: Investment costs of low power thermal absorption chillers.

The calculated solar thermal energy prices are between 85 € MWh^{-1} and 258 € MWh^{-1} for solar cooling applications, depending on the operating hours and the location. They go down as far as 76 € MWh^{-1} for an office in Madrid with high internal loads and a high temperature cooling distribution system. These costs are getting close to economic operation compared with fossil fuel heating supply.

Depending on control strategy and building type, the total costs for a solar thermal absorption cooling system in a Southern European location such as Madrid/Spain are between $170 - 320 \text{ € MWh}^{-1}$. If the system integration and mounting costs are assumed to be 45% of total investment costs instead of 17%, the costs per MWh of cold are in the range of $300 - 390 \text{ € MWh}^{-1}$ for an office in Madrid with low internal loads and 200 € MWh^{-1} for the best case of an office with longer operating hours (see figure 27).

In the case of an absorption chiller connected to a district heating system, heat prices can be lowered while the costs associated to the system components (mostly chiller and cooling tower) remain the same. A case study was done for a 105 kW Yazaki WFC-SC 30 absorption chiller connected to a 6 MW biomass powered district heating network in Ostfildern/Germany. The cost of the absorption chiller itself are only 25% of the total capital costs (see figure 28). With a heat price of 20 € MWh^{-1} , total cooling costs for 2000 full load hours are 169 € MWh^{-1} . 62% of the cooling costs are capital costs, 10% are operating costs and 28% are energy costs. At electricity costs of 120 € MWh^{-1} the specific costs for a corresponding vapor-compression chiller with a COP of 4 would be approximately 115 € MWh^{-1} .

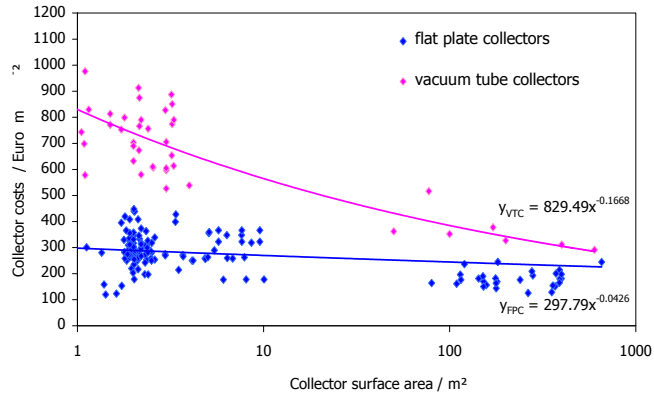


Figure 22: Specific collector costs without VAT as a function of size of the installation.

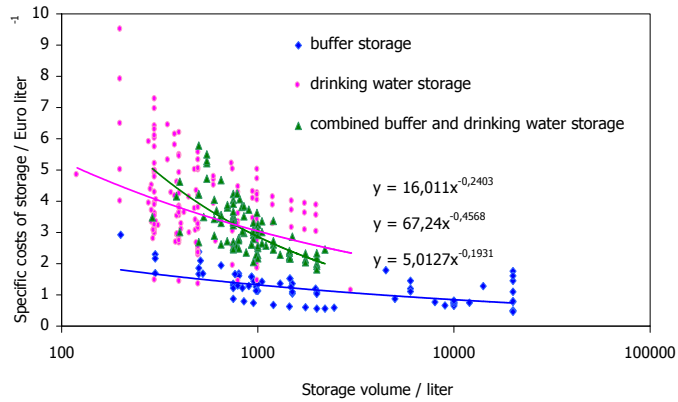


Figure 23: Costs for different storage tank sizes and systems.

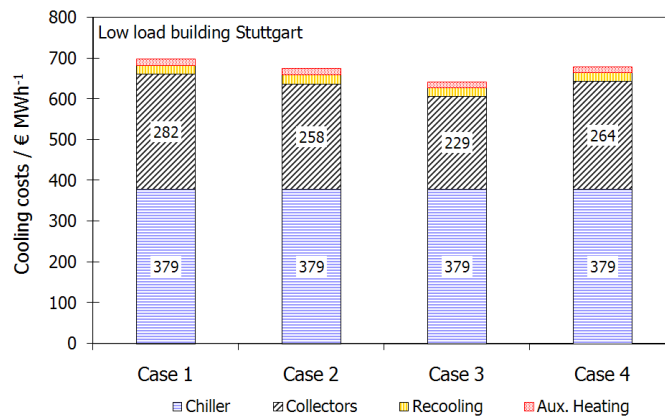


Figure 24: Cooling costs per MWh of cold for different system technology options and control strategies. Low load building Stuttgart.

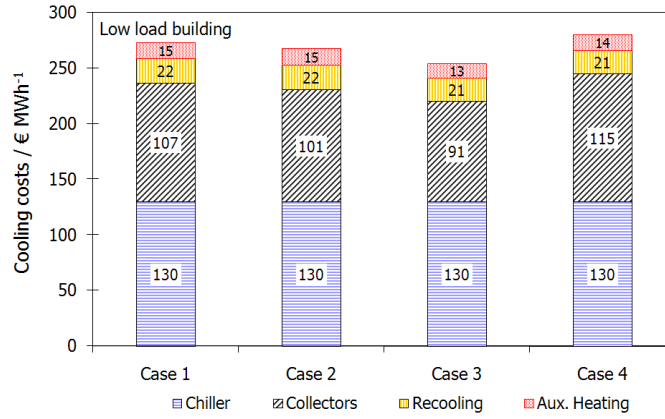


Figure 25: Cooling costs per MWh of cold for different system technology options and control strategies. Low load building Madrid

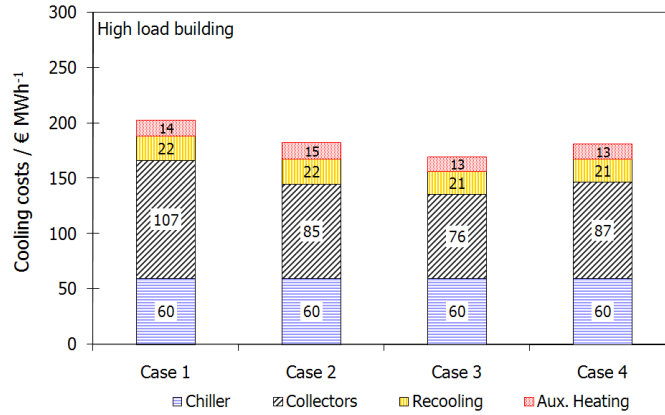


Figure 26: Cooling costs for different operation strategies and cooling distribution systems for the office with high internal loads. High load building Madrid

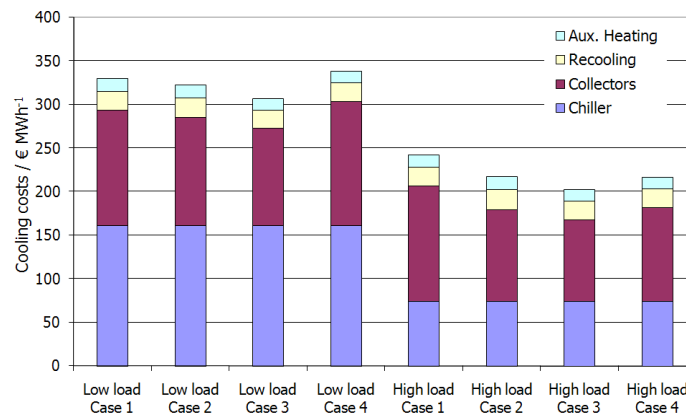


Figure 27: Cost distribution for a solar thermal absorption chiller system with mounting and integration costs of 45% of total investment cost.

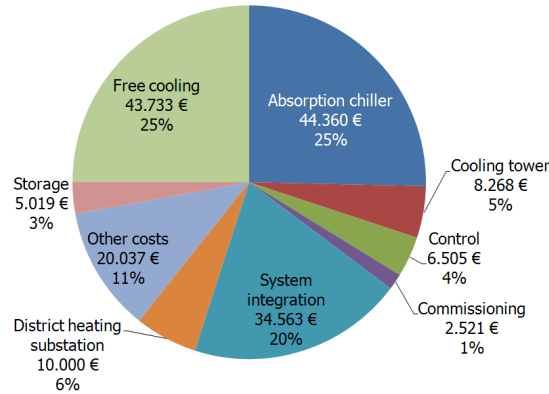


Figure 28: Distribution of capital costs of an absorption cooling system connected to a district heating network including a free cooling system.

By comparison, Schölkopf (2004) calculated the cost of conventional cooling systems for an energy efficient office building in Germany to be 180 € per MWh. 17% of the cost were for the electricity consumption of the chiller. The total annual cooling energy demand for the 1094 m² building was 31 kWh m⁻²a⁻¹. Own comparative calculations for a 100 kW thermal cooling project showed that the compression chiller system costs without cold distribution in the building were between 110 and 140 € per MWh.

Henning (2004) also investigated the costs of solar cooling systems compared to conventional technology. The additional costs for the solar cooling system per MWh of saved primary energy were between 44 € per MWh in Madrid and 77 € per MWh in Freiburg for large hotels. It is clear that solar cooling systems can only become economically viable, if both the solar thermal and the absorption chiller costs decrease. This can be partly achieved by increasing the operation hours of the solar thermal system and thus the solar thermal efficiency by also using the collectors for warm water production or heating support.

Costs of desiccant cooling systems

The costs for desiccant cooling units are often full system costs, as the desiccant unit already includes parts of the conventional distribution system such as fans, fresh air channels, exhaust air channels, filters etc. Furthermore, the machine itself contains humidifiers and heat exchangers, which are also available when a conventional air handling unit is installed.

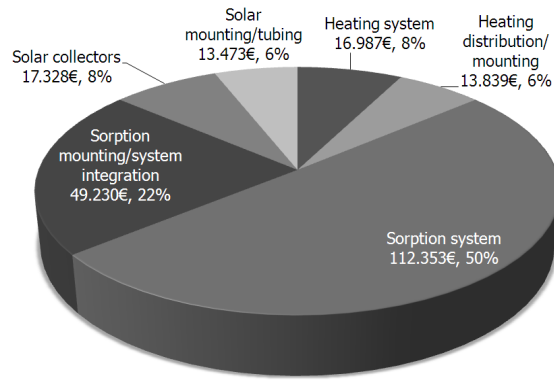


Figure 29: Total investment costs for hardware, tubing and system integration for the solar powered desiccant cooling plant in Althengstett with 18.000 m³/h volume flow.

As an example the total capital, consumption and operation related costs were analysed for the Althengstett demonstration system with a volume flow of 18.000 m³ h⁻¹. The investment costs are dominated by the desiccant unit itself and its system integration, which together cause 72% of the total investment costs. The solar air collector field including tubing and mounting contributes to only 14% of the total investment costs at 300 Euro per square meter collector area (see figure 29). The total investment costs per m³ h⁻¹ are 12.4€. For another well analysed system of the IHK in Freiburg/Germany with a smaller volume flow of 10 000 m³ h⁻¹ the costs were higher at 16.6€ per m⁻³ h⁻¹. Also in this system, the DEC unit together with the air channels, mounting and control caused about 2/3 of the total investment costs (46% for the unit itself, 17% for mounting and channels and 6% for control). The solar air collector field was responsible for 10% of the total costs (Hindenburg, 2002). A third system with 105 m² solar air collectors connected in series to a ventilated photovoltaic facade and shed roof was constructed in Mataró, Spain with a total volume flow of 12 000 m³ h⁻¹. As a part of a European Union demonstration project, the unit was constructed in Germany and then mounted and connected to the existing building management system by the Spanish project partners. Here the DCS unit caused 33% of the total costs of 179 300 €, and a high amount of 23% were used for the unit control and its connection to the existing building management system. The collectors were responsible for 12% of the total investment costs, but mounting and system integration was expensive at 15%. In total the price per cubic meter and hour of air flow was similar to the German system with 15 € per m³ h⁻¹.

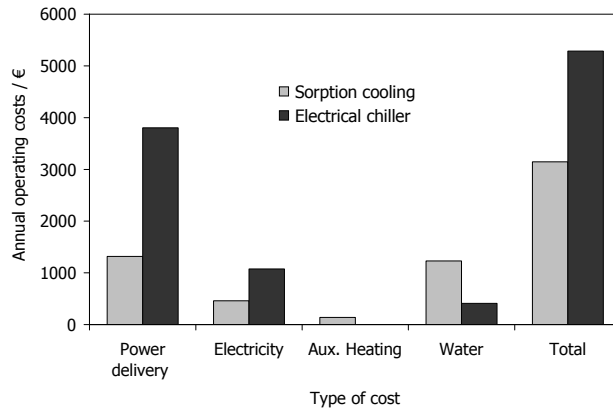


Figure 30: Annual consumption costs for the installed desiccant cooling system compared to an electrical chiller.

From the total investment costs in the Maier factory project, an annuity of 26 070 € capital related costs results. If the funding for the DEC investment costs of 100.000 € is taken into account, the annuity reduces to 14 122 €. Consumption related costs for heat, electricity and water consumption occur together with the demand charge to provide a given electrical power. In total the annual consumption costs for the desiccant cooling system were calculated with 3147 €, about 40% less than for a conventional air conditioning system (see figure 30). In the Spanish Mataró project, the savings calculated from electrical peak power cost reduction were 4200 € per year.

In addition operation related costs for maintenance and repair occur. Repair costs are usually between 1 and 3% of investment costs, for the calculations, 2% were chosen. Maintenance costs are in a similar range. 76% of the total annual costs are capital costs, the rest is for operation and consumption costs (see figure 31).

The annual heating energy saving through the solar thermal collector field of about 1500 € can be subtracted from the total annual costs. The remaining cooling costs for the investigated year with 34 710 kWh of cold production result in a specific cold price of 0.94 € per kWh without funding and 0.6 € per kWh including the investment funding. By comparison, the costs for a conventional air handling unit with humidification and an electrical compression chiller were calculated in this project with 0.65 € per kWh. The high price per Kilowatt hour is largely due to the low total cooling demand in the building. At a nominal power of the system of approximately 100 kW, the cooling energy corresponds to only about 350 full load hours. In climates with higher cooling demand and 1000 load hours, the

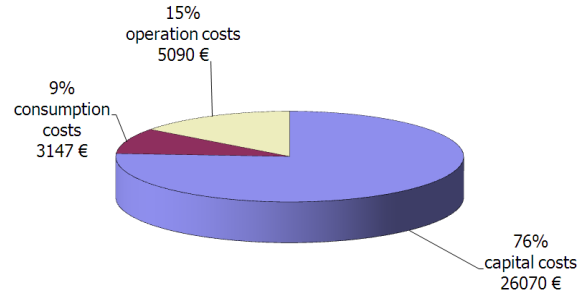


Figure 31: Distribution of total annual costs for the installed system including subsidy on the capital costs.

price could then go down to 0.3 € per kWh. An Austrian research team compared the costs of a district heating powered small DEC system ($6000 \text{ m}^3 \text{ h}^{-1}$) with an air handling unit with an electrical compression chiller. For 960 full load hours, they obtained cooling costs for the DEC unit of about 0.55 € per kWh compared to 0.51 to 0.56 € per kWh for the electrical cooling system (depending on the tariff structure). Also here the capital costs are about $2/3$ of the total annual costs of the system (Simader, Rakos, 2005).

Conclusions

The paper gives an overview of the two main technologies used in solar thermal cooling systems, namely closed cycle absorption chillers and open desiccant cooling systems. While absorption chillers can be used in a wide range of applications with cold distribution based on water or air systems, desiccant cooling systems are mainly recommendable if the needed fresh air flow is high in a building. For all solar thermal cooling technologies, the reduction auxiliary electrical energy consumption is a major goal, as otherwise primary energy savings are not significant. This means an optimised control strategy especially for partial load operation and good design of the heat source and heat sink circuits. The surface area of solar thermal collectors for an absorption cooling system strongly depends on the full load hours of the system. For building with low internal loads, about 2 m^2 per kilowatt cooling power are sufficient to achieve 80% solar fraction, for buildings with high loads and up to 2000 full load hours, about 4 m^2 per kW are recommended.

The total system costs for commercially available solar cooling systems in a Southern European location are between 180 – 320 € MWh⁻¹, depending on the cooling load file and the chosen control strategy. The total costs are dominated by the costs for the solar thermal system and the chiller itself. For a more moderate climate such as Germany with a low cooling energy demand, the costs rise to 680 € MWh⁻¹.

In desiccant cooling systems, capital costs clearly dominate the total costs. About 2/3 of the investment costs are due to the desiccant air conditioning and distribution system, while the solar collectors are just 10 - 15% of the investment. Per m³ h⁻¹ volume flow the investment costs are between 12 - 17 €. Depending on the full load hours, this results in a cooling price between 300 and 900 € MWh⁻¹. In moderate climates, the number of regeneration hours with solar thermal operation is limited, as often evaporative cooling is sufficient. Here the specific collector summer yield is rather low and new control strategies need to be found to optimise the solar thermal contribution.

Acknowledgements

We acknowledge the financial support of the European Union within the project POLYCITY, contract TREN/05FP6EN/S07.43964/51381.

The authors like to thank the following colleagues from the research centre zafh.net at the University of Applied Sciences Stuttgart: Martin Huber, who provided the building load files using TRNSYS and Juergen Schumacher, who supported the solar cooling modelling work in INSEL. The description of the history of solar cooling systems is taken from the PhD work of Dr. Uli Jakob. The analysis of the desiccant cooling system in Althengstett was carried out in the PhD work of Dr. Uwe Schürger. The analysis of the district heating absorption chillers was done by Eric Duminiil.

References

- [1] Albers, J., Ziegler, F., Analysis of the part load behaviour of sorption chillers with thermally driven solution pumps, Proceedings of the 21st IIR International Congress of Refrigeration, August 17-22, International Institute of Refrigeration (IIR), Washington D.C., USA, ISBN

- [2] Assilzadeh, F., Kalogirou, S.A., Ali, Y., Sopian, K., Simulation and optimisation of a LiBr solar absorption cooling system with evacuated tube collectors, *Renewable Energy*, Vol. 30, 1143 - 1159, 2005
- [3] Atmaca, I., Yigit, A., Simulation of solar-powered absorption cooling system, *Renewable Energy* 28, 2003
- [4] Beccali, M., Butera, F., Guanella, R., Adhikari, R.S. (2003) Simplified models for the performance evaluation of desiccant wheel dehumidification, *International Journal of Energy Research*, Vol. 27, pp 17 – 29
- [5] Bujedo L., Rodriguez, J., Marticnez, P.J., Rodriguez, L.R., Vicente, J., Comparing different control strategies and configurations for solar cooling, *Proceedings EUROSUN 2008*, 7th to 8th October, Lisbon, Portugal (2008)
- [6] Davanagere, B.S., Sherif, S.A., Goswami, D.Y. (1999) A Feasibility study of solar desiccant air conditioning system - Part I: psychrometrics and analysis of the conditioned zone, *International Journal of Energy Research*, Vol. 23, pp 7 – 21
- [7] Engler, M., Grossmann, G., Hellmann, H.-M., Comparative simulation and investigation of ammonia-water: absorption cycles for heat pump applications, *Int. J. Refrig.*, Vol 20, No 7, pp 504-516, 1997
- [8] EAW, Absorptionskälteanlage Wegracal SE 15 – Technische Beschreibung (Absorption Chiller Wegracal SE 15 – technical description). Company product information. EAW Energieanlagenbau GmbH, Germany, 2003
- [9] Eicker, U., *Solar Technologies for Buildings* (2003) John Wiley and Sons Ltd, ISBN 0-471-48637-X
- [10] Eicker, U., Pietruschka, D., Design and performance of solar powered absorption cooling systems in office buildings, *Energy and Buildings* (2008), doi: 10.1016/j.enbuild.2008.07.015

- [11] Florides, G.A., Kalogirou, S.A., Tassou, S.A., Wrobel, L.C., Modelling, simulation and warming impact assessment of a domestic-size absorption solar cooling system, *Applied Thermal Engineering*, Vol 22, No 12, 2002
- [12] Gao, Z., Viung, C.M., Tomlinson, J.J. (2005) Theoretical analysis of dehumidification process in a desiccant wheel, *Heat Mass Transfer* 41, pp 1033 – 1042
- [13] Gassel, A. (2004) *Kraft-Wärme-Kälte-Kopplung und solare Klimatisierung*, Habilitationsschrift TU Dresden
- [14] Ginestet, S. Stabat, P., Marchio, D. (2003) Control design of open-cycle desiccant cooling systems using a graphical environment tool, *Building Service Engineering Research and Technology*, Vol. 24, No. 4, 257-269
- [15] Grossmann, G. (2002) Solar powered systems for cooling, dehumidification and air conditioning, *Solar Energy* Vol. 72, pp53-62
- [16] Henning, H.-M. *Solar-assisted air-conditioning in buildings – a handbook for planners*, Springer-Verlag 2004, ISBN 3-211-00647-8
- [17] Henning, H.-M., *Solare Klimatisierung - Stand der Entwicklung* Fraunhofer-Institut für Solare Energiesysteme ISE Tagung Solares Kühlen, Wirtschaftskammer Österreich, Wien, 7.5.2004
- [18] Hindenburg, C. *Anlagenplanung und Betrieb einer offenen sorptionsgestützten Klimaanlage*, Proceedings of 2nd Symposium Solares Kühlen in der Praxis, HFT Stuttgart, 2002
- [19] Hoeper, F. (1999). *Optimierte Anlagenschaltung zur solaren Kühlung mit Absorptionstechnik* (Optimised design for solar cooling with absorption refrigeration units). *KI Luft- und Kältetechnik*. Vol. 35, No. 8, pp. 397-400. ISSN 0945-0459.
- [20] INSEL 7.0 Block reference manual, www.insel.eu
- [21] Jakob, U., Eicker, U., Taki, A.H., Cook, M.J., Development of an optimised solar driven Diffusion-Absorption Cooling Machine, Proceedings of the ISES Solar World Congress 2003, June 16-19, International Solar Energy Society (ISES), Göteborg, Sweden, ISBN 91-631-4740-8, 2003

- [22] Jakob, U. (2005). Investigations into Solar Powered Diffusion-Absorption Cooling Machines. PhD Thesis. De Montfort University Leicester
- [23] Kanoğlu, M., Bolattürk, A., Altuntop, N. (2007) Effect of ambient conditions on the first and second law performance of an open desiccant cooling process, *Renewable Energy* Volume 32, Issue 6, pp 931-946
- [24] Kim, D.S., Machielsen, C.H.M., Evaluation of air-cooled solar absorption cooling systems, ISHPC '02, Proceedings of the International Sorption Heat Pump Conference, Shanghai, China, September 24-27, 2002
- [25] Kimura, K. (1992). Solar Absorption Cooling. in SAYIGH, A.A.M. (Edit.) and MCVEIGH, J.C. *Solar Air Conditioning and Refrigeration* (1st ed.). Oxford: Pergamon Press Ltd., England. pp. 13-65. ISBN 0-08-040750-1.
- [26] Kim, D.S., Wang, L., Machielsen, C.H.M. (2003) Dynamic modelling of a small-scale NH₃/H₂O absorption chiller, Proceedings of the 21st IIR International Congress of Refrigeration, August 17-22, International Institute of Refrigeration (IIR), Washington D.C., USA, ISBN 2-913149-32-4, 2003
- [27] Kohlenbach, P. "Solar cooling with absorption chillers: Control strategies and transient chiller performance", Dissertation Technische Universität Berlin, 2007
- [28] Lamp, P. and Ziegler, F. (1997). Solar Cooling with closed Sorption Systems. Proceedings of the Workshop Solar Sorptive Cooling. 16th-17th October, Forschungsverbund Sonnenenergie (FVS), Hardthausen, Germany. pp. 79-92. ISSN 0949-1082.
- [29] Loewer, H. (1978). Solar-Kühlung in der Klimatechnik (Solar refrigeration for air conditioning installations). *Ki Klima-Kälte-Ingenieur*. Vol. 6, No. 4, pp. 155-162. ISSN 0340-398X.
- [30] Maclaine-Cross, I.L. (1988) Proposal for a desiccant air conditioning system, *ASHRAE Transactions* 94 (2), pp1997 – 2009

- [31] Mei, V.C., Chen, F.C., Lavan, Z., Collier, R.K., Meckler, G. (1992), An assessment of desiccant cooling and dehumidification technology, Report prepared by the Oak Ridge National Laboratory, Contract No. DE-AC05-84OR21400
- [32] Mendes, L.F, Collares-Pereira, M., Ziegler, F. (1998) Supply of cooling and heating with solar assisted heat pumps: an energetic approach”, *Int. J. Refrig.* Vol 21, No.2, pp 116-125
- [33] Mittal, V., Kasana, K. S., Thakur, N.S, Performance evaluation of solar absorption cooling system of Bahal (Haryana), *HJ. Indian Inst. Sci*, Sept.-Oct., Vol 85, 295-305, 2005.
- [34] Nick-Leptin, Joachim (2005). Political framework for research and development in the field of renewable energies, *International Conference Solar Air conditioning*, Staffelstein 2005
- [35] Panaras, G., Mathioulakisa, E., Belessiotisa, V. (2007). Achievable working range for solid all-desiccant air-conditioning systems under specific space comfort requirements. *Energy and Buildings*, Volume 39, Issue 9, pp 1055-1060
- [36] Pennington, N.A. (1955) Humidity Changer for Air Conditioning, U.S. patent No. 2,700,537.
- [37] Pietruschka, D., Jakob, U., Eicker, U., Hanby, V. Simulation based optimisation and experimental investigation of a solar cooling and heating system, *Proceedings of the Solar air conditioning*, 2nd international conference, Tarragona, Spain, 2007
- [38] Pietruschka, D., Jakob, U., Eicker, U., Hanby, V., Simulation based optimisation of a newly developed system controller for solar cooling and heating systems, *Proceedings EUROSUN 2008*, 7th to 8th October, Lisbon, Portugal (2008)
- [39] Preisler, Anita (2008). ROCOCO – Final Report, Project n°TREN/05/FP6EN/SO7.54855/020094
- [40] Schumacher, J. (1991) *Digitale Simulation regenerativer elektrischer Energieversorgungssysteme*, Dissertation Universität Oldenburg, 1991 www.insel.eu
- [41] Safarik, M., Weidner, G. (2004). Neue 15kW H₂O-LiBr Absorptionskälteanlage im Feldtest für thermische Anwendungen (New 15kW H₂O-LiBr Absorption Cooling Machine in field test for

- thermal applications). Proceedings of the 3rd Symposium Solares Kühlen in der Praxis. Fachhochschule Stuttgart - Hochschule für Technik, Germany. Vol. 65, pp. 159-171.
- [42] Schweigler, C., Storckenmaier, F., Ziegler, F, Die charakteristische Gleichung von Sorptionskälteanlagen, Proceedings of the 26th Deutsche Klima-Kälte-Tagung, Berlin, Germany, 1999
- [43] Schoelkopf, W., Kuckelkorn, J., Verwaltungs- und Bürogebäude – Nutzerverhalten und interne Wärmequellen, OTTI Kolleg Klimatisierung von Büro- und Verwaltungsgebäuden, Regensburg 9/2004
- [44] Simader, G., Rakos, C. Klimatisierung, Kühlung und Klimaschutz: Technologien, Wirtschaftlichkeit und CO2 Reduktionspotentiale. Austrian Energy Agency, Vienna 2005
- [45] Storckenmaier, F., Harm, M, Schweigler, C., Ziegler, F., Alebers, J., Kohlenbach, P., Sengewald, T. (2003). Small-Capacity Water/LiBr Absorption Chiller for Solar Cooling and Waste-Heat Driven Cooling. Proceedings of the 21st IIR International Congress of Refrigeration. 17th-22nd August, International Institute of Refrigeration (IIR), Washington D.C., USA. ISBN 2-913149-32-4.
- [46] Sumath, K., Study on a solar absorption air-conditioning system, Proceedings of the International Congress of Refrigeration, Washington, D.C., USA, 2003
- [47] Yasuo Takagi, Tadashi Nakamaru and Yoshihiko Nishitani, an absorption chiller model for HVAC-SIM+, Toshiba corporation, proceedings of the international building performance simulation association, 1999
- [48] Tommy, H.J.M. (1994), Simulation of a PV-Diesel Generator Hybrid System and Investment Analysis: Case Study of a Mountain Hostel, Master Thesis, Renewable Energy Group, Department of Physics, Carl von Ossietzky University Oldenburg, Germany
- [49] Wardono, B., Nelson, R.M., Simulation of a double effect LiBr/H₂O Absorption Cooling System, ASHRAE Journal pp 32-38, October 1996

- [50] Willers, E., Neveu, P., Groll, M., Kulick, C., Meunier, F., Mostofizadeh, C., Wierse, M., Dynamic modelling of a liquid absorption system, ISHPC '99, Proceedings of the International Sorption Heat Pump Conference, Munich, Germany, March 24-26, 1999
- [51] Ziegler, F. , Sorptionswärmepumpen, Forschungsberichte des Deutschen Kälte- und Klimatechnischen Vereins Nr. 57, Stuttgart, ISBN 3-932715-60-8, 1998
- [52] Ziegler, F. (1999). Recent developments and future prospects of sorption heat pump systems. Int. J. Therm. Sci.. Vol. 38, pp. 191-208. ISSN 1290-0729.